Nuclear Inst. and Methods in Physics Research, A 961 (2020) 163673

Contents lists available at ScienceDirect

Nuclear Inst. and Methods in Physics Research, A

journal homepage: www.elsevier.com/locate/nima

Minimizing distortions with sectored GEM electrodes

A.P. Marques [a,b], F.M. Brunbauer [a,*], H. Müller [a], R. de Oliveira [a], E. Oliveri [a], D. Pfeiffer [a,c], L. Ropelewski [a], J. Samarati [a,c], F. Sauli [a], L. Scharenberg [a,d], L. Shang [e], M. van Stenis [a], S. Williams [a], Y. Zhou [f]

[a] European Organization for Nuclear Research (CERN), CH-1211 Geneve 23, Switzerland
[b] Department of Physics, University of Coimbra, Rua Larga, 3004-516 Coimbra, Portugal
[c] European Spallation Source (ESS ERIC), P.O. Box 176, SE-22100 Lund, Sweden
[d] University of Bonn, Regina-Pacis-Weg 3, 53113 Bonn, Germany
[e] State Key Laboratory of Solid Lubrication, Lanzhou Institute of Chemical Physics, Chinese Academy of Science, Lanzhou, 730000, China
[f] State Key Laboratory of Particle Detection and Electronics, University of Science and Technology of China, Hefei 230026, China

ARTICLE INFO

Keywords:
GEM
Sectorization
Sectors
Distortions
DLC

ABSTRACT

Electrode sectorization is an important design principle for large area GEM based detectors. It reduces the energy of discharges and permits to disconnect defective or shorted sectors, but induces a local signal distortion and a potential efficiency loss. We implemented and evaluated a new design approach for the insulating gaps between electrode sectors, to minimize or mitigate distortions and dead regions. By preserving the hole pattern of GEMs even in the insulating region between electrode sectors, the response of the detector in these regions was partly recovered resulting in reduced distortions. Single-side sectored GEMs were optically read out to study the influence of different sectorization patterns. Recorded images show a clear improvement with full holes both aligned with the rows and with a random alignment as compared to the traditional blank insulating strip between sectors. A sectored GEM manufactured on a substrate coated with a resistive DLC layer was evaluated and shown to minimize distortions. The investigated sectorization patterns provide a way of recovering signals in the insulating or resistive regions between sectors in GEM-based detectors.

1. Introduction

Gaseous Electron Multipliers (GEMs) [1] consist of an insulating polyimide foil that is metal-coated on both sides and patterned with a high density of chemically etched holes. When applying a suitable voltage difference between the two electrodes, the electric field in the holes is high enough to achieve electron avalanche multiplication. Thanks to its high gain, robustness and reliability, this type of gas detectors is widely used in high energy physics experiments like COMPASS [2], LHCb [3], TOTEM [4], KLOE-2/DAFNE [5] and BM@N [6]. In addition to operational experiments, several upgrade projects involving GEM detectors are currently ongoing. This includes an upgrade of the CMS muon system [7] as well as a GEM-based readout for the ALICE TPC [8]. GEMs are also used on other systems requiring good position resolution in the detection of ionizing radiation for charged particles, photons, X-rays and neutrons, and also in medical applications and dosimetry for radiation therapy [9].

In the infrequent but possible case of a discharge, the energy stored in large area GEMs with a high capacitance may have a destructive effect on the foils [10]. Discharges can also propagate to anodes and damage readout electronics. Sectorization of GEMs can overcome this problem by partitioning the active surface into several sectors, which are individually powered through protection resistors, thus reducing the energy of subsequent discharges, due to its lower capacity. Therefore, sectorization has become a standard technique and is applied in many experimental setups, as for muon detection in the large area GEMs for the on-going CMS upgrade [7,11].

Despite its benefits, sectorization results in signal distortion and loss of efficiency in the region of the insulating gap between sectors. Such distortions were already observed in the triple-GEM tracking detector for COMPASS [12]. While this may be corrected in tracking applications relying on the redundancy of multiple detection layers, it might be unacceptable for demanding imaging applications.

Sectorization is typically achieved by introducing an insulating region without holes between two electrode sectors on one side of a GEM foil. In this region, the metal is removed and the insulating substrate (polyimide) is exposed. The width of such insulating gaps is around 100–200 μm, resulting in a distortion of the electric field in this region. Electrons moving towards the GEM foil may be lost or collected into the holes of the adjacent electrode sectors and therefore deviated from their original paths. This standard design for sector gaps on the

* Corresponding author.
E-mail address: florian.brunbauer@cern.ch (F.M. Brunbauer).

https://doi.org/10.1016/j.nima.2020.163673
Received 22 November 2019; Received in revised form 14 February 2020; Accepted 17 February 2020
Available online 19 February 2020

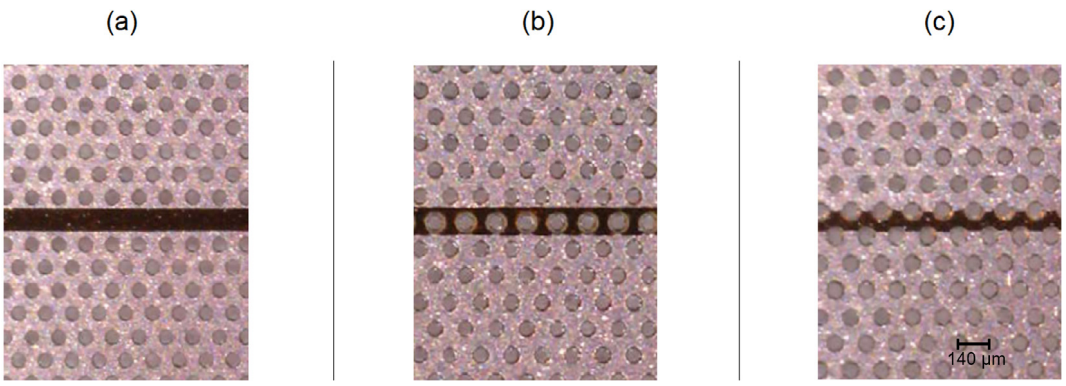

Fig. 1. Microscope pictures of the different sectorization patterns: (a) blank strip, (b) full aligned holes and (c) random holes. The opposite side of the foil is not sectored.

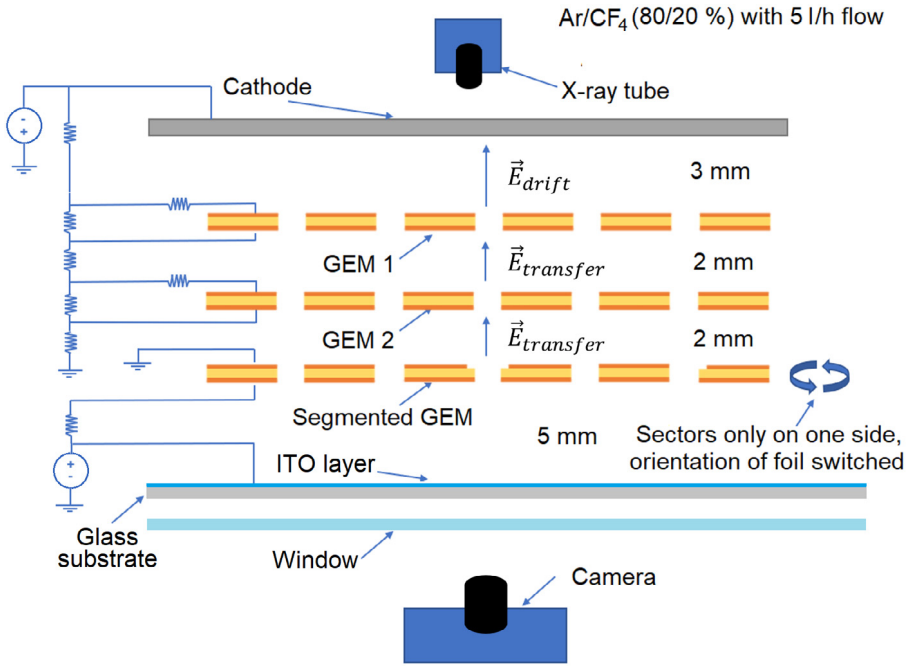

Fig. 2. Detector configuration and X-ray irradiation setup.

sectored side of a GEM foil is shown in Fig. 1(a). The width of the sector gap was 120 µm in all investigated foils.

To minimize the distortions at the sector gaps, we tested an alternative design preserving the hole pattern also in the insulating region (Fig. 1(b)). While electrode sectorization is preserved by removing the metal along a strip, the hole pattern is not perturbed and holes are present also in the insulating gap. Although the electric field is distorted in this region, this design may result in some electric field lines leaking through the holes in the insulating region. This allows some electrons to follow their initial trajectories and undergo multiplication when traversing the GEM in the regions between adjacent electrode sectors.

In addition to the standard geometry with no holes in the sector gap (blank strip, Fig. 1(a)) and with holes in the gap, which is aligned with the hole pattern (full holes, Fig. 1(b)), we also investigated the effect of a random alignment of the hole pattern and the sector gap (random holes, Fig. 1(c)). This solution simplifies the manufacturing of large size foils, as it does not require a precise alignment of the gap with the rows of holes.

In addition to preserving the hole pattern in the insulating gaps to allow electrons to traverse the GEM foils in these regions, a resistive coating in the sector gaps restoring the electric field may reduce or eliminate distortions and allow efficient electron multiplication in the sector gaps. We used a polyimide foil, coated on one side with a resistive Diamond-Like Carbon (DLC) layer before metallization, and etching to ensure the same electrical potential across the GEM, including in the gap region.

2. Experimental setup and methods

A triple-GEM detector with an active area of 10 × 10 cm^2 was operated in an Ar/CF_4 (80/20%) gas mixture at atmospheric pressure with a flow of 5 l/h. We used standard GEMs with double-conical holes with a diameter of 70 µm and a pitch of 140 µm, which were produced with the double-mask technique. The first two GEMs in the stack had non-sectorized electrodes and the last GEM had a sectored electrode on one side with 4 rectangular sectors with a size of 2.5 × 10 cm^2 each. An Al foil was used as cathode and an ITO-coated glass plate as anode. A drift region with a thickness of 3 mm between the first GEM and the cathode was used. The transfer gaps between GEM foils were set at 2 mm. The thickness of the induction gap was 5 mm. The detector was placed in a gas volume with an acrylic window.

We studied the detector under X-ray irradiation with a Cu target tube. Scintillation light emitted during electron avalanche multiplication [13] was optically read out as shown in Fig. 2 to acquire images of the response of the detector at the sector gaps. The close-up images of

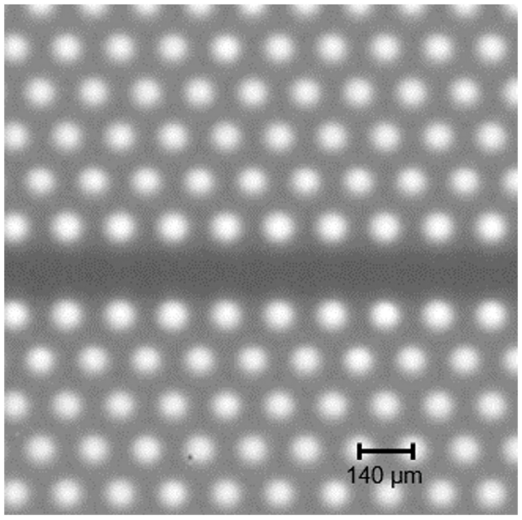

Fig. 3. Optically read out image of the blank strip of a sectorized GEM under X-ray irradiation.

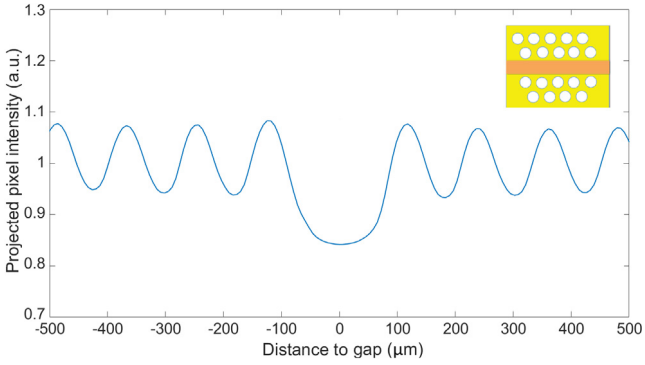

Fig. 4. Projected pixel intensity for blank strip pattern in the sectorized GEM.

the detector response show the hexagonal hole pattern with the holes being the locations of scintillation light emission. Images were recorded with an exposure time of 10 s per frame, using a low-noise CCD camera (QImaging Retiga R6 [14]) with a resolution of 6 megapixels. Ten frames were averaged per image. An averaged background image, acquired with the sectorized GEM powered off, was subtracted to remove the contribution of the first two GEMs to the observed scintillation light intensity. Thus, the presented images show only the scintillation light emitted in the sectorized GEM.

A lens with a focal length of 50 mm and additional collimating lenses resulted in a magnification factor of about 1.5 and an effective pixel size of 6.5×6.5 μm on the image plane. This high resolution pixelated readout allowed a detailed study of the light emission profile from individual holes of the GEM and the localization and quantification of electron avalanche multiplication.

The effect of the orientation of the single-side sectorized GEM foils was investigated by reversing their orientation. The two geometries are conventionally named "sectors at bottom" when they face the anode, and "sectors at top" when they face the other GEMs.

After recording the images, we obtained a 1-dimensional projection of the pixel intensity as a function of the distance from the sectorized region, to quantify the light emission in this region while comparing with the continuous electrode region. The procedure consists of summing up the intensities of all pixels in a horizontal line and repeating this in the orthogonal direction along the recorded image. Subsequently, the obtained values were normalized to a mean value obtained from averaging over several holes at a large distance from the gap, which were not affected by it.

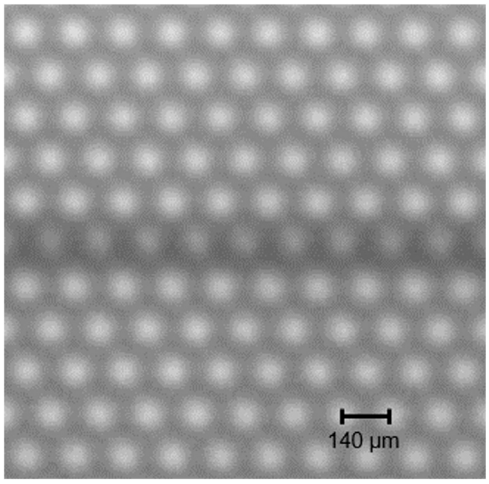

Fig. 5. Optically read out image of the full holes with standard substrate GEM under X-ray irradiation.

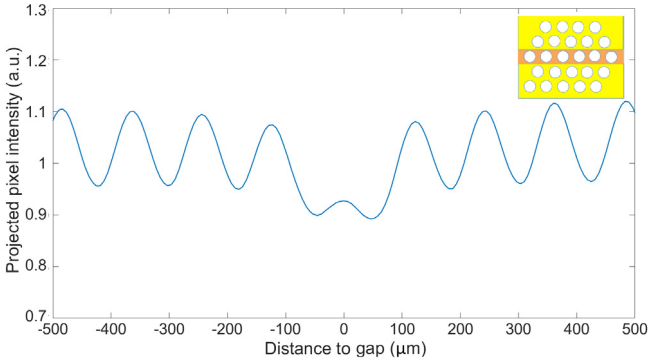

Fig. 6. Projected pixel intensity for full holes pattern in the sectorized GEM.

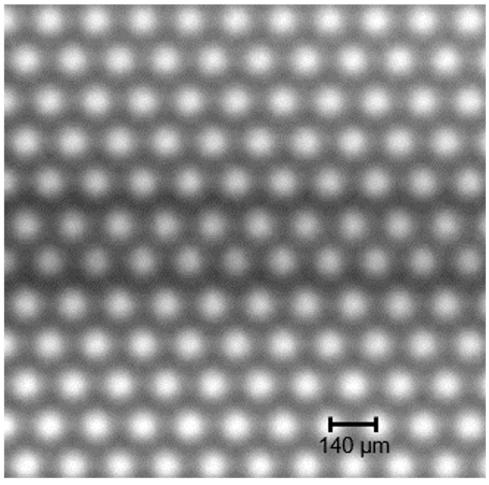

Fig. 7. Optically read out image of the random holes GEM under X-ray irradiation.

3. Results and discussion

3.1. Blank sector gap

An optically read out image of the response of the GEM with the blank strip under X-ray irradiation is shown in Fig. 3. The sectored side was at the bottom facing the anode. With this standard sectorization

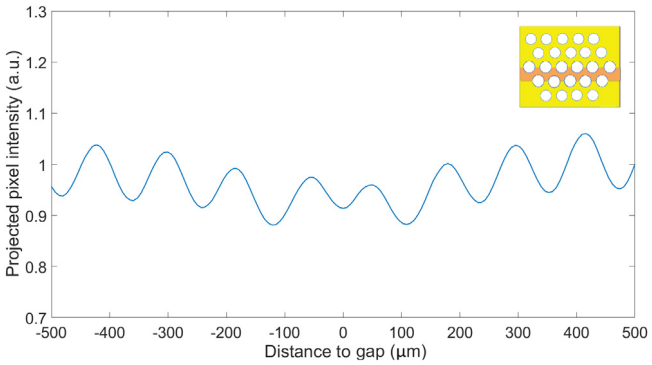

Fig. 8. Projected pixel intensity for random holes pattern in the sectorized GEM.

pattern, the difference between the continuous electrode and the sector region is noticeable.

To quantify differences in the distortion caused by different sector designs, a 1-dimensional projection is shown in Fig. 4. A significant drop in the pixel intensity is observed at the sector gap. There is a small increase of intensity in the peaks adjacent to the gap that is attributed to a redistribution of a fraction of the electrons from the sectorized region to the neighbouring holes.

The non-zero observable signal around the gap region in Fig. 4 might be explained by reflections or direct light from the tip of the avalanches outside the holes. The light emission profile from a single GEM hole was optically recorded and determined to have a Gaussian shape. The width of the emission profile from a single hole does not explain the residual light signal between holes or in the blank gap region [15]. This observation favours an explanation involving the reflection of light from the electrodes or the window of the gas volume but will be studied in further measurements.

3.2. Full holes in sector gap

An image of the response of a GEM with full holes in the sector gap is shown in Fig. 5. The sectored side was at the bottom facing the anode. In contrast to the dark region in the blank strip case, the holes in the sector gap are visible in the optically read out image. This is attributed to some electrons traversing these holes and contributing to the observed light signal by undergoing avalanche multiplication. This observation confirms that having holes in the sectorized region may reduce the distortion in this region.

Fig. 6 shows the projected pixel intensity along the GEM. Albeit of lower intensity, a signal in the gap is visible, which corresponds to the contribution of holes in the sector gap to the recorded signal.

The presence of holes in the sector gap thus recovers some signal in this region reducing the observed losses. While the signal in the gap regions is significantly lower than the one inside the electrodes, the presence of a residual signals allows offline correction of the response. Thus, response maps of the GEM can be used to minimize distortions in imaging applications.

3.3. Random holes in sector gap

A third design without any particular alignment between the hole pattern and sector gap was studied. In this so called “random” alignment case, the relative location of the hole pattern with respect to the sector gap changes across the area of the GEM. This results in some regions with alignment resembling the full holes case, while in other areas the sector gap lies in-between rows of holes. The sectored side was at the bottom facing the anode.

Although the random alignment case results in some holes which are partially surrounded by metal, no adverse effect on the operation and stability of the GEM foils was observed. The maximum achievable voltage before the onset of instabilities was similar in all three investigated designs.

The response of the detector in the vicinity of a sector gap is shown in Fig. 7.

The sector gap affects the response of two rows of holes with a smaller distortion on each one than in the full holes design. The difference between the full holes and the random alignment is more visible with the 1-dimensional projection of the pixel intensity shown in Fig. 8. There is a reduction in the distortion in the sectorized region, but there is also a decrease in the signal intensity for the rows of holes adjacent to the gap. Thus, it appears that the random alignment results in a distribution of the distortion around the sector gap to a wider region.

3.4. Full holes in DLC-coated sector gap

We studied a sectored GEM based on a DLC-coated substrate, to further minimize the distortion in the sector gap. The substrate was a polyimide foil with a DLC layer with a sheet resistance of about 1 GΩ/square on one side, which was deposited by magnetron sputtering [16]. Copper layers were added to each side of the foil with thin Cr layers for adhesion. A 3D model of the DLC-coated GEM is presented in Fig. 9. The DLC layer is present across the full foil and is only exposed in the sector gaps. This composite foil was subsequently structured as a GEM with sectorization on the side of the DLC coating. A 3 MΩ was measured between adjacent sectors which suggests that the sheet resistivity was in fact higher than the nominal one.

This GEM with resistive DLC layers between electrode sectors was characterized in the same way as described above. Its response is shown in Fig. 10. With the sectors at the bottom, the response resembles the one of the full hole case. However, for the opposite orientation, corresponding to the sectors on the top, significantly higher light emission in the holes in the sector gap was observed as shown in Fig. 10(a). This top orientation of the sectors produces an image with almost no noticeable distortion.

The response in the two orientations is compared in the 1-dimensional projection of pixel intensity shown in Fig. 11. In the bottom orientation, the DLC does not seem to behave in a significantly different way compared to the full hole design. In the top orientation, the two adjacent peaks around the gap have a slightly lower intensity compared to all other peaks and it seems that this slight decrease is compensated by the increase in the peak in the sector gap region.

The recorded 1-dimensional projections were numerically integrated to quantify the total scintillation light emitted. We chose and compared three different regions in the 1-dimensional projection plots

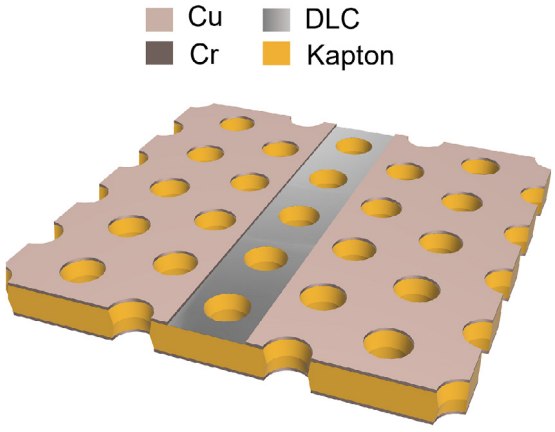

Fig. 9. 3D model of the DLC-coated GEM.

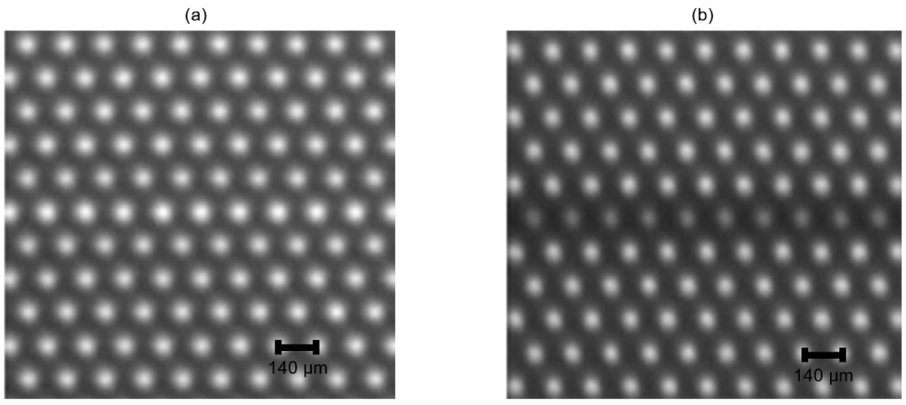

Fig. 10. Optically read out image of the full holes with DLC GEM under X-ray irradiation with sectors at (a) top and (b) bottom.

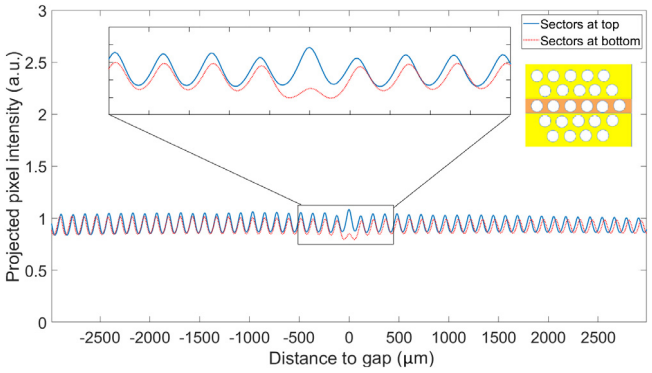

Fig. 11. Projected pixel intensity for full holes pattern in the DLC GEM.

to investigate if there is any signal loss in the region surrounding the sector gap. An offset was subtracted from the data. The resulting plots and integrated areas are shown in Fig. 12.

As shown in Fig. 12(a), the integrated value of the pixel intensity around the sector gap was significantly lower in the bottom orientation than in the regions within the electrodes, on the left and right sides of the gap. For the sectors at top orientation, shown in Fig. 12(b), no significant difference in the in integrated values could be observed when comparing regions well withing the electrodes and the region centred around the sector gap.

The difference for the two orientations may be explained by potentially different hole geometries on the two sides. These may arise from the process used to manufacture the holes pattern in the presence of the DLC layer, which cannot be etched in the same way as metals. The observed difference cannot be explained by thickness variations due to the manufacturing process of the copper electrodes on the two sides of the GEM [17].

4. Conclusions

We investigated alternative designs of the insulating gaps between electrode sectors of GEMs. Preserving the hole pattern in the sector gap of sectorized GEMs allows the partial recovery of the signals in this region allowing to reduce the distortions caused by sectorization. Both the full hole design and the random alignment appeared to be superior to the conventional blank strip case. While the intensity of the recovered signals in the sector gap region is lower, it might be corrected by an offline algorithm using a response map for imaging applications.

The random alignment between sector gaps and the hole pattern was effective in reducing distortions, while permitting a simpler way to the sectorize GEM electrodes. The precise alignment of the sector gap with respect to the hole pattern, as realized in the full hole case, was possible for a small area GEM. However, it may not be feasible for larger foils. In addition, this may also be used to create sector gaps that cannot be aligned with the hole pattern. An example of this are the circular sectors used for the so-called planispherical GEM with sectored electrodes [18]. The present study shows that it may be possible to retain the hexagonal hole pattern across the full active area and structure sector gaps arbitrarily without taking into account the hole pattern. Preliminary tests suggest that the stability of this design is similar to the one of the design with an aligned hole pattern and sector gaps. However, this still needs to be studied conclusively.

Using DLC as resistive layer in the sector gaps achieves results comparable to the other evaluated designs if sectors are at the bottom side. In the top orientation, a higher signal level is observed in the holes in the sector gap. The difference between the top and bottom orientations in the case of the GEM based on a DLC-coated foil requires further investigations.[1] As the process of structuring GEM holes in a

[1] It should be noted that the sectors on top is the solution adopted by most systems, based on considerations on the prevention of discharge propagation [2].

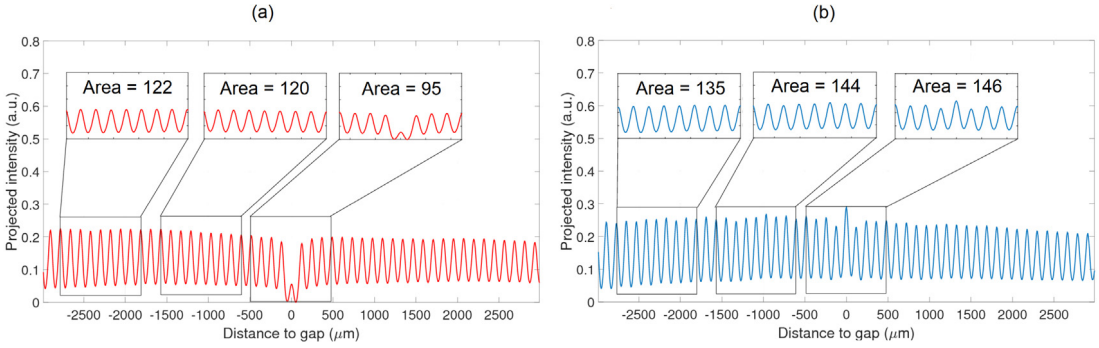

Fig. 12. Integration results for bottom orientation (a) and top orientation (b).

DLC-coated substrate is relatively new compared to standard Cu electrode GEMs, the hole geometry and quality should be further optimized. Charging-up effects of sector gaps were not studied and remain the subject of further investigations.

The described sectorization designs provides a potential solution to the distortions observed for large area GEM foils. Thus, it may be possible to achieve a more uniform response across sectorized GEMs and use this approach for demanding imaging applications.

CRediT authorship contribution statement

A.P. Marques: Conceived and designed the analysis, Collected the data, Contributed data or analysis tools, Performed the analysis, Wrote the paper. **F.M. Brunbauer:** Conceived and designed the analysis, Collected the data, Contributed data or analysis tools, Performed the analysis, Wrote the paper. **H. Müller:** Conceived and designed the analysis. **R. de Oliveira:** Collected the data. **E. Oliveri:** Conceived and designed the analysis. **D. Pfeiffer:** Conceived and designed the analysis. **L. Ropelewski:** Conceived and designed the analysis. **J. Samarati:** Conceived and designed the analysis. **F. Sauli:** Conceived and designed the analysis, Collected the data, Contributed data or analysis tools, Performed the analysis, Wrote the paper. **L. Scharenberg:** Conceived and designed the analysis. **L. Shang:** Collected the data. **M. van Stenis:** Collected the data. **S. Williams:** Collected the data. **Y. Zhou** Collected the data.

Declaration of competing interest

The authors declare that they have no known competing financial interests or personal relationships that could have appeared to influence the work reported in this paper.

References

[1] F. Sauli, GEM: A new concept for electron amplification in gas detectors, Nucl. Instrum. Methods Phys. Res. A 386 (2) (1997) 531–534, http://dx.doi.org/10.1016/S0168-9002(96)01172-2.

[2] B. Ketzer, S. Bachmann, M. Capeans, M. Deutel, J. Friedrich, S. Kappler, I. Konorov, S. Paul, A. Placci, K. Reisinger, L. Ropelewski, L. Shekhtman, F. Sauli, GEM detectors for COMPASS, IEEE Trans. Nucl. Sci. 48 (4) (2001) 1065–1069, http://dx.doi.org/10.1109/23.958724.

[3] A. Cardini, G. Bencivenni, P. Simone, The operational experience of the triple-GEM detectors of the LHCb muon system: Summary of 2 years of data taking, in: IEEE Nuclear Science Symposium Conference Record, 2012, pp. 759–762, http://dx.doi.org/10.1109/NSSMIC.2012.6551204.

[4] M. Bozzo, M. Oriunno, L. Ropelewski, F. Sauli, R. Orava, J. Ojala, K. Kurvinen, R. Lauhakangas, J. Heino, W. Snoeys, F. Ferro, M. Van Stenis, E. David, Design and construction of the triple GEM detector for TOTEM, in: IEEE Symposium Conference Record Nuclear Science 2004, vol. 1, 2004, pp. 447–450, http://dx.doi.org/10.1109/NSSMIC.2004.1462231.

[5] M. Silarski, The KLOE-2 experiment at DAFNE, in: A. Wroska, A. Magiera, C. Guaraldo, H. Ströher (Eds.), EPJ Web Conf. 130 (2016) 01020, http://dx.doi.org/10.1051/epjconf/201613001020.

[6] A. Galavanov, M. Kapishin, K. Kapusniak, V. Karjavine, S. Khabarov, Y. Kirushin, A. Kolesnikov, E. Kulish, V. Lenivenko, A. Makankin, A. Maksymchuk, B. Mehl, R. Oliveira, V. Plotnikov, G. Pokat, A. Rodriguez, M. Rumyantcev, I. Rufanov, V. Sidorenko, A. Vishnevskiy, Performance of the BM@N GEM/CSC tracking system at the Nuclotron beam, EPJ Web of Conf. 204 (2019) 07009, http://dx.doi.org/10.1051/epjconf/201920407009.

[7] A. Colaleo, A. Safonov, A. Sharma, M. Tytgat, CMS Technical Design Report for the Muon Endcap GEM Upgrade, Tech. Rep. CERN-LHCC-2015-012. CMS-TDR-013, CERN, 2015, URL https://cds.cern.ch/record/2021453.

[8] A. Mathis, ALICE Collaboration, From gated to continuous readout - the GEM upgrade of the ALICE TPC, in: Proceedings, 5th International Conference on Micro Pattern Gas Detectors (MPGD2017): Temple University, Philadelphia, USA, May 22–26, 2017, PoS MPGD2017 (2019) 055, http://dx.doi.org/10.22323/1.322.0055.

[9] F. Sauli, The gas electron multiplier (GEM): Operating principles and applications, in: Special Issue in memory of Glenn F. Knoll, Nucl. Instrum. Methods Phys. Res. A 805 (2016) 2–24, http://dx.doi.org/10.1016/j.nima.2015.07.060.

[10] S. Bachmann, A. Bressan, M. Capeáns, M. Deutel, S. Kappler, B. Ketzer, A. Polouektov, L. Ropelewski, F. Sauli, E. Schulte, L. Shekhtman, A. Sokolov, Discharge studies and prevention in the gas electron multiplier (GEM), Nucl. Instrum. Methods Phys. Res. A 479 (2002) 294–308, http://dx.doi.org/10.1016/S0168-9002(01)00931-7.

[11] D. Abbaneo, C. Armagnaud, M. Abbrescia, P. Aspell, S. Bally, Y. Ban, L. Benussi, U.M.R. Berzano, S. Bianco, J. Bos, K. Bunkowski, J. Cai, J. Chatelain, J. Christiansen, A. Colaleo, C. Garcia, E. David, R. Oliveira, M. Zientek, GEM based detector for future upgrade of the CMS forward muon system, Nucl. Instrum. Methods Phys. Res. A 718 (2013) 383–386, http://dx.doi.org/10.1016/j.nima.2012.10.058.

[12] C. Altunbas, M. Capéans, K. Dehmelt, J. Ehlers, J. Friedrich, I. Konorov, A. Gandi, S. Kappler, B. Ketzer, R.D. Oliveira, S. Paul, A. Placci, L. Ropelewski, F. Sauli, F. Simon, M. van Stenis, Construction, test and commissioning of the triple-GEM tracking detector for COMPASS, Nucl. Instrum. Methods Phys. Res. A 490 (1) (2002) 177–203, http://dx.doi.org/10.1016/S0168-9002(02)00910-5.

[13] F. Brunbauer, M. Lupberger, E. Oliveri, F. Resnati, L. Ropelewski, C. Streli, P. Thuiner, M. van Stenis, Radiation imaging with optically read out GEM-based detectors, J. Instrum. 13 (02) (2018) T02006, http://dx.doi.org/10.1088/1748-0221/13/02/t02006.

[14] Qimaging, Teledyne QImaging retiga r6 CCD camera for fluorescence imaging, 2019, URL https://www.qimaging.com/retiga-r6.

[15] A. Marques, Summer Student Project Report, CERN Summer Students Reports, Sep 2019, URL http://cds.cern.ch/record/2690697/files/Summer_Student_Project_Report.pdf?version=1&fbclid=IwAR0kc5cD7h91i4n7SFRG9Q4a0Ea2M3NEyI71QQLwbruGqZraZveySDC8bj0.

[16] Y. Lv, Y. Zhou, J. Liu, M. Shao, Z. Zhang, G. Song, X. Wang, Production and performance study of diamond-like carbon resistive electrode in MPGD, Nucl. Instrum. Methods Phys. Res. A (2019) 162759, http://dx.doi.org/10.1016/j.nima.2019.162759.

[17] D. Janssens, A better understanding of the gas gain in GEM detector, RD51 Collaboration Meeting, Oct 2019, URL https://indico.cern.ch/event/843711/contributions/3556737/attachments/1929547/3195468/DjunesJanssens_RD51_CERN.pdf.

[18] F. Brunbauer, E. Oliveri, F. Resnati, L. Ropelewski, F. Sauli, P. Thuiner, M. van Stenis, The planispherical chamber: A parallax-free gaseous X-ray detector for imaging applications, Nucl. Instrum. Methods Phys. Res. A 875 (2017) 16–20, http://dx.doi.org/10.1016/j.nima.2017.08.060.